Sensor Data Fusion for Seamless Navigation using Wi-Fi Signal Strengths and GNSS Pseudoranges

Philipp Richter[1], Jochen Seitz[2], Lucila Patiño-Studencka[1], Javier Gutierréz Boronat[1], Jörn Thielecke[2]

[1]Fraunhofer Institute IIS Nuremberg, Germany
[2]University of Erlangen-Nuremberg, Germany

Abstract

This paper proposes an information fusion approach for seamless indoor and outdoor positioning in urban scenarios. In these scenarios the global navigation satellite systems (GNSS) easily reach their limitations, whereas Wi-Fi fingerprinting positioning systems profit from signal degradation such as shadowing and reflection. The solution presented here is based on a Bayesian framework, fusing data from a Wi-Fi fingerprinting algorithm with pseudoranges of a GNSS receiver. A particle filter is used to combine the Wi-Fi database correlation results computed on a discrete fingerprint grid with the pseudorange measurements. Further, the additional estimation of the GNSS user clock offset, allows this approach to be seen as a Wi-Fi aided position, velocity and time determination algorithm (PVT) of a GNSS receiver. The presented algorithm has the ability to improve the Wi-Fi fingerprinting algorithm with less than four pseudoranges available. A filter to solve the typical Wi-Fi fingerprint positioning ambiguities has been developed. This algorithm achieves a higher robustness and accuracy, compared to standalone Wi-Fi positioning or GNSS, especially in urban canyon scenarios.

Index Terms

positioning, sensor data fusion, particle filter, wi-fi fingerprinting, global navigation satellite system

I. Introduction

Since its proliferation and mass-market penetration, GNSSs have been used to locate their users all over the world. GNSS is the first choice of system used for navigation and localisation. Although, better GNSS position accuracies have been achieved through the use of multi-frequency receivers and the help of assisted data, errors caused by environmental obstructions, such as signal blocking and multipath phenomena, remain and are the most challenging. To overcome these problems, promising approaches using sensor data fusion have come up. This paper focuses on filtering methods that increase the position accuracy of GNSS and allow a seemless indoor-outdoor localisation with the help of wireless LAN (Wi-Fi™ (Wi-Fi, n.d.)).

GNSS is based on time-of-arrival measurements. These are translated to distances to the satellites, better known as *pseudoranges*. Therefore GNSS receivers need a line-of-sight to the satellites to compute an adequate user position. The presented method of incorporating Wi-Fi signals relies on *fingerprinting* as a method of Wi-Fi positioning (Bahl & Padmanabhan, 2000). The advantage of using Wi-Fi, in particular a Wi-Fi fingerprinting positioning system, lies in its position accuracy, scalability, large deployment of access points and especially in its complement errors in comparison to the errors of GNSSs: GNSSs (receivers) perform best in open areas with line of sight to as many satellites as possible and degrade in urban environments and indoors. In contrast, the Wi-Fi fingerprinting positioning systems benefit from signal shadowing, caused by obstacles and reflections. Obstructions of any kind give a more distinguishable radio map and therefore less ambiguous position estimates. On the other hand, Wi-Fi fingerprinting positioning accuracy decreases in open areas, where shadowing effects are scarce.

A few studies on sensor data fusion of GNSS and Wi-Fi exist. In (Mok & Lau, 2001) and (Mok & Xia, 2005), MEREA is presented as a method to combine ranges to local road points (e.g. range to a Wi-Fi access point (AP)) and pseudoranges to get a position fix when less than 4 satellites are available. This idea was further developed by (Li *et al.* , 2011) as a method to improve Wi-Fi positioning with only two satellites in view. In (Shah & Malaney, 2006) intermittent GNSS positions were integrated into a particle filter to increase tracking accuracy in Wi-Fi networks. A pure position based fusion of GNSS and Wi-Fi fingerprinting was presented in (Eck *et al.* , 2012). And finally a Wi-Fi assisted GPS (Wi-Fi-A-GPS) has been published in (Weyn & Schrooyen, 2008), in order to reduce the time-to-first-fix. However, all systems

relying on GNSS positions have the drawback that a reliable integrity measure is needed and hardly achieved, which easily worsen the solution.

Our approach fuses GNSS pseudoranges and the correlation results of the probabilistic Wi-Fi fingerprinting proposed by (Wallbaum & Wasch, 2004) via a sequential Bayesian estimator. *Measurement models*, which relate the observations to the state of the systems, are defined and presented by probability density functions. A pseudoranges likelihood function is used to represent the GNSS measurements, whereas, in the case of Wi-Fi measurements, a *pseudo-likelihood* is constructed, based on the Wi-Fi fingerprint correlation results. The combination of the measurement likelihoods is then the key of the sensor data fusion. By estimating not only the position, but also the velocity and time offset of the receiver, a Wi-Fi aided PVT is hereby developed. This ubiquitous filter framework allows seamless positioning, indoors and outdoors, and provides the possibility to comprise different *system models* depended on the dynamic of the system. To account for multimodal distributions, and to address possibly non-Gaussian distributions a particle filter is chosen, to compute the Bayesian solution. The originality of this paper lies in the data fusion of continuous pseudoranges with received signal strength indicators (RSSI), evaluated on a discrete grid. The deep integration of the sensor data achieves a Wi-Fi aided GNSS PVT, which is able to provide a positioning with less than 4 satellites in view.

The reminder of the paper is organised as follows: Beginning in section II with a general description of the Bayesian framework for localisation. Section III presents the system and the measurement models within the construction of likelihoods. Section IV covers the realisation of the estimator via particle filter, followed by section V, which explains the conducted experiments and its results and covers general performance, drawbacks and possibilities of the newly proposed algorithm.

II. Bayesian Filtering for Positioning

Consider the movement of an object as a dynamic, stochastic process possessing an internal state. The problem is to estimate the location of a mobile user (MU), for instance a pedestrian, for each time step $k = 1, 2, \ldots$, based on GNSS pseudorange- and/or Wi-Fi RSSI measurements. The *state vector*, describing the internal state, at time k is denoted as $\mathbf{x}_k \in \mathbf{X}_k$, with $\mathbf{X}_k$ the *state space*. Assuming the dynamic of the system to be Markovian, it can generally be represented by

$$\mathbf{x}_k = \mathsf{f}(\mathbf{x}_{k-1}, \mathbf{u}_k) \tag{1a}$$

$$\mathbf{z}_k = \mathsf{g}(\mathbf{x}_k, \mathbf{v}_k). \tag{1b}$$

$\mathsf{f}(\cdot)$ and $\mathsf{g}(\cdot)$ describe the generic state space model and are possibly non-linear functions. With $\mathbf{z}_k$ the vector of measurements, $\mathbf{u}_k$ and $\mathbf{v}_k$, denote possibly non-Gaussian noise variables. (1a) describes the transition from the last state to the current state, and (1b) describes how the measurements are related to the system state. The optimal Bayesian filter for this case is given below.

Given the past measurements $\mathbf{z}_{1:k} = \{\mathbf{z}_1, \ldots, \mathbf{z}_k\}$ at time k, the recursive Bayesian estimator updates the so-called *aposteriori* probability distribution function (PDF) $p(\mathbf{x}_k \mid \mathbf{z}_{1:k})$ over time as follows (Gordon *et al.* , 1993):

$$p(\mathbf{x}_k \mid \mathbf{z}_{1:k-1}) = \int f(\mathbf{x}_k \mid \mathbf{x}_{k-1}) p(\mathbf{x}_{k-1} \mid \mathbf{z}_{1:k-1}) \mathsf{d}\mathbf{x}_{k-1} \tag{2a}$$

$$p(\mathbf{x}_k \mid \mathbf{z}_{1:k}) = \frac{g(\mathbf{z}_k \mid \mathbf{x}_k) p(\mathbf{x}_k \mid \mathbf{z}_{1:k-1})}{\int g(\mathbf{z}_k \mid \mathbf{x}_k) p(\mathbf{x}_k \mid \mathbf{z}_{1:k-1}) \mathsf{d}\mathbf{x}_k}. \tag{2b}$$

Assuming the posterior PDF of time $k-1$ is known, the prior PDF can be predicted with help of the system model described by the state transition PDF $f(\mathbf{x}_k \mid \mathbf{x}_{k-1})$. The result $p(\mathbf{x}_k \mid \mathbf{z}_{1:k-1})$ is then corrected by measurements, represented by their likelihood functions $g(\mathbf{z}_k \mid \mathbf{x}_k)$. The denominator of the posterior PDF (2b) is a normalising constant. A solution to the sequential Bayesian estimator is usually yielded by the mode or mean of the posterior PDF. (2a) is usually referred as *apriori* probability density function. For further details, see e.g. (Arulampalam *et al.* , 2002).

III. Process and Sensor Models

According to a position, velocity and time algorithm (PVT) of a GNSS receiver, the state vector

$$\mathbf{x}_k = (\mathbf{p}_k, \dot{\mathbf{p}}_k, t_k, \dot{t}_k)^T$$

corresponds to the position $\mathbf{p} = (\mathsf{x}, \mathsf{y}, \mathsf{z})^T$ and velocity $\dot{\mathbf{p}} = (\dot{\mathsf{x}}, \dot{\mathsf{y}}, \dot{\mathsf{z}})^T$ of the MU. Additionally it includes the receiver time offset with respect to GNSS time t and its derivative $\dot{t}$. The next subsection describes in detail the model for the system itself and the models involved in the pseudorange measurements and the probabilistic database correlation. The state vector itself is defined on a *state space* $\mathbf{X}$.

A. Process model

The dynamics of the MU is modelled according to a pedestrian without any further knowledge about its movements. A Langevine process was chosen to model the MU motion. It was successfully applied to similar problems (Vermaak & Blake, 2001) and it performed better than a constant velocity model, especially for pedestrians, with usually slow and unsteady dynamics. The one dimensional discrete Langevine model in x as stated below:

$$\mathsf{x}_k = \mathsf{x}_{k-1} + \Delta T \dot{\mathsf{x}}_k \tag{3}$$

$$\dot{\mathsf{x}}_k = a_{\mathsf{x}} \dot{\mathsf{x}}_{k-1} + b_{\mathsf{x}} u_{\mathsf{x},k}, \qquad u_{\mathsf{x}} \sim \mathcal{N}(0,1) \tag{4}$$

ΔT corresponds to the time interval separating two consecutive updates of the filter, and $a_{\mathsf{x}} = \exp(-\beta_{\mathsf{x}} \Delta T)$, $b_{\mathsf{x}} = \bar{\nu}_{\mathsf{x}} \sqrt{1 - a_{\mathsf{x}}^2}$. The model parameter $\bar{\nu}$ is the steady state velocity, and β is the rate constant of the process. The excitation process u_{x} is standard normal distributed. This model accounts for many kinds of motions and basically increases the variance of the position estimate.

The GNSS receiver clock is modelled according to (Bradford *et al.* , 1996) as a random walk,

$$t_k = t_{k-1} + \dot{t}_{k-1} \Delta T + q_k \qquad q_k \sim \mathcal{N}(0, \sigma_q) \tag{5}$$

$$\dot{t}_k = \dot{t}_k + w_k \qquad w_k \sim \mathcal{N}(0, \sigma_w) \tag{6}$$

with additive uncorrelated Gaussian noise.

As a result, we can summarise the process model in a linear equation

$$\mathbf{x}_k = \mathbf{A}\mathbf{x}_{k-1} + \mathbf{B}\mathbf{u}_k. \tag{7}$$

B. GNSS Pseudorange Model

In order to correct the state vector, the prior PDF (2a) respectively, a likelihood function for the pseudorange measurements must be established.

Let ϱ_k^j be a pseudorange constructed by a GNSS receiver for each satellite $j = 1, \ldots, J$ at time k. According to (Bradford *et al.* , 1996) it can be modelled as

$$\begin{aligned} \varrho_k^j &= ||\mathbf{p}_{s_k}^j - \mathbf{p}_k|| + t_k + \varepsilon_k^j \\ &= \sqrt{(\mathsf{x}_{s_k}^j - \mathsf{x}_k)^2 + (\mathsf{y}_{s_k}^j - \mathsf{y}_k)^2 + (\mathsf{z}_{s_k}^j - \mathsf{z}_k)^2} + t_k + \varepsilon_k^j \end{aligned}$$

Where $\mathbf{p}_k$ represents the receiver (MU) location, the satellite location is denoted by $\mathbf{p}_{s_k}^j$, and $\varepsilon_k = \mathcal{N}(0, \sigma_\varepsilon)$ summarises other errors of each satellite to MU link, which are not further considered at this stage of the research. Recall (5) and (6) for the model of t_k.

A detailed description of the concept of GNSS can be found in (Bradford *et al.* , 1996).

Following (Khider *et al.* , 2010), we establish the pseudorange likelihood function as Gaussian variable. By assuming independence of pseudoranges and noise of each satellite, we can give the likelihood function for all satellites as the product of single likelihood functions.

$$\begin{aligned} p(\boldsymbol{\varrho}_k \mid \mathbf{x}_k) &= \prod_{j=1}^{J} \frac{1}{\sqrt{2\pi}\sigma_\varepsilon^j} \exp\left(\frac{\varrho_k^j - \hat{\varrho}_k^j}{\sigma_\varepsilon^j} \right)^2 \\ &= \frac{1}{\sqrt{2\pi}\sigma_\varepsilon} \exp\left(\frac{\boldsymbol{\varrho}_k - \hat{\boldsymbol{\varrho}}_k}{\sigma_\varepsilon} \right)^2. \end{aligned} \tag{8}$$

C. Wi-Fi RSSI Model

Wi-Fi fingerprinting is conceptually based on the idea that each environment has unique signal propagation characteristics. So assume that each location can be associated with a unique tuple of signal strength from each Wi-Fi access point. Wi-Fi fingerprinting consists of two phases; i) the calibration phase and ii) the positioning phase. The first one consists of creating a *radio map* as a prerequisite to the positioning phase. Its empiric approach, focused on, can be considered to be a collection of calibration points at different locations. For each calibration point a tuple of RSSI is measured from visible access points, and stored in a database. In phase ii), once again, RSSI readings from each available AP are measured and compared with all database entries to determine the closest match. The best match leads to the most probable position.

Challenging are the database entries, with similar fingerprints, i.e. similar tupels of RSSI readings. To tackle that issue, (Wallbaum & Wasch, 2004), (Seitz *et al.* , 2010a) and Seitz *et al.* (2010b) suggest a probabilistic database correlation. This approach is followed in this paper, and their sensor model to compare the RSSI measurements with the radio map, is used.

The fingerprints are taken on discrete positions to establish the radio map. These discrete positions are defined on the (state) space $\breve{\mathbf{X}} \subseteq \mathbb{R}^3$, which consists of $\mathrm{dom}(\breve{\mathbf{X}}) = \breve{\mathbf{x}}^1 \cup \breve{\mathbf{x}}^2 \cup \cdots \cup \breve{\mathbf{x}}^M$ regions of equal volume. $m = 1, 2, \ldots, M$ denotes the number of regions. Each region has a volume $|\breve{\mathbf{x}}^m|$ to which a probability can be assigned. Under the condition that all volumes $|\breve{\mathbf{x}}^m|$ are the same size, a region can be approximated by its mean $\bar{\mathbf{p}}^m$. The interested reader is referred to (Thrun *et al.* , 2006). Now, the fingerprint database can be established, e.g. consisting of $\{\mathrm{ID}^m, \bar{\mathbf{p}}^m, \mathbf{s}^m\}_{m=1}^M$, in which $\mathbf{s}^m$ describes a RSSI tuple of L measurements at location $\bar{\mathbf{p}}^m$. With $l = 1, \ldots, L$, the number of APs is denoted and ID^m is a vector containing an identification for each AP.

Let's assume that the RSSI tuple is received at time instance k, with the readings from all L APs, be denoted as $\mathbf{s}_k = s_k^1, s_k^2, \ldots, s_k^L$. The probabilistic correlation of received RSSI with a RSSI value of the radio map $\hat{s}^{m,l}$, of which the product over all APs is taken, is given by

$$\Pr(\mathbf{s}_k \mid \mathbf{x}_k) = \int_{s_k^l - \Delta s}^{s_k^l + \Delta s} \prod_{l=1}^{L} \frac{1}{\sqrt{2\pi}\sigma_\kappa^l} \exp\left(-\frac{1}{2}\left(\frac{s_k^l - \hat{s}^{m,l}}{\sigma_\kappa^l}\right)^2\right) \mathrm{d}\mathbf{s}. \tag{9}$$

It expresses the conditional probability of a RSSI measurement obtained at a certain location $\mathbf{X}_k = \mathbf{x}_k$, and it might be referred to as a probabilistic correlation result. In other words, it reflects the state $\mathbf{x}_k$ via the measured RSSI tuple $\mathbf{s}_k$ and its entry in the fingerprint database $\mathbf{s}^m$. The closer the measured RSSI tuple to the radio map RSSI entry, the higher the likelihood that the measurement was conducted at the according radio map location entry. The notation of the variance for the noise of the Wi-Fi links is σ_κ^l. In the empiric Wi-Fi fingerprinting it can be considered as a filter parameter to describe the environment or scenario and hence is constant. In the literature the keyword "location variability" can be found. The integration is usually carried out over the RSSI range of 1 dB, and hence Δs is chosen according to that. For that discussion see also (Wallbaum & Wasch, 2004).

The proposed pseudo-likelihood will then be defined by the probabilities of each entry of the radio map. After normalising these correlation results, they are united to a discrete probability map, i.d. to a probability mass function over $\breve{\mathbf{X}}_k$. From now on we will refer to this pseudo-likelihood function as

$$p(\mathbf{s}_k \mid \mathbf{x}_k) = \int_{\mathcal{S}} \frac{1}{\sqrt{2\pi}\sigma_\kappa} \exp\left(-\frac{1}{2}\left(\frac{\mathbf{s}_k - \hat{\mathbf{s}}^m}{\sigma_\kappa}\right)^2\right) \mathrm{d}\mathbf{s}. \tag{10}$$

IV. Algorithm Design

Considering the nature of our problem, the integrals of the optimal Bayesian filter unfortunately do not have a closed form solution. Accordingly to the presented models a particle filter is chosen to approximate Bayes recursion. Particle filter are sequential Monte Carlo methods which have been employed in many signal processing areas (Arulampalam *et al.* , 2002). For practical reasons, we use the SIR particle filter as in (Gordon *et al.* , 1993).

The SIR particle filter is conceptually simple, straightforward to implement and has moderate computational requirements, which is the reason it is applied here.

The general idea behind a particle filter is that it approximates PDFs with a set of N samples and their according weights, $\{\mathbf{x}_k^i, \omega_k^i\}_{i=1}^N$.

$$p(\mathbf{x}) = \sum_{i=1}^{N} \omega_k^i \delta(\mathbf{x}_k - \mathbf{x}_k^i)$$

Assume that the sought posterior PDF is known; one could directly draw particles from it and assign a weight equal to $1/N$ to each particle. But given that direct sampling from $p(\mathbf{x}_k \mid \mathbf{z}_{1:k})$ is impossible, the concept of *importance sampling* applies here. With respect to importance sampling the weights are updated by

$$\omega_k^i = \frac{g(\mathbf{z}_k \mid \mathbf{x}_k^i) f(\mathbf{x}_k^i \mid \mathbf{x}_{k-1}^i)}{q(\mathbf{x}_k^i \mid \mathbf{x}_{k-1}^i, \mathbf{z}_k)} \omega_{k-1}^i,$$

with $q(\cdot)$ denoting the importance density and $g(\cdot)$ the likelihood function. Furthermore, the weights need to be normalised such that $\sum_i \omega_k^i = 1$. With this approximation, integrals are converted into sums and these can be evaluated straightforward.

The SIR particles filter has two main characteristics. One, that the importance density equals the transition probability density function. The other, that the particles will be resampled after each recursion. By applying these two characteristics to importance sampling, it follows the unnormalised weights

$$\tilde{\omega}_k^i = g(\mathbf{z}_k \mid \mathbf{x}_k^i).$$

It states that only the likelihood functions are necessary to update the weights. The weights are normalised by $\omega_k^i = \tilde{\omega}_k^i / \sum_{n=1}^{N} \tilde{\omega}_k^n$.

The sought PDFs are given by (2) to solve our problem. Assume an initial PDF is available, where the initial set of particles $\mathbf{x}_0^i$ can be sampled from and to which equal weights $\omega_0^i \leftarrow 1/N$ are assigned. A probabilistic particle representation of the state transition PDF is given by the process model,

$$f(\mathbf{x}_k^i \mid \mathbf{x}_{k-1}^i) \sim \mathcal{N}(\mathbf{x}_k; \mathbf{A}\mathbf{x}_{k-1}, \mathbf{B}\mathbf{B}^T).$$

Therefore, a particle approximation of the prior PDF (2a) can be computed by propagating the set $\mathbf{x}_k^i$ through the transition equation (7).

Moving forward on Bayesian recursion (2b), the posterior density function needs to be evaluated.

Due to the independence of the measurement likelihood functions (8) and (10), it is reasonable to let

$$g(\mathbf{z}_k \mid \mathbf{x}_k^i) = p(\mathbf{s}_k \mid \mathbf{x}_k^i) \cdot p(\boldsymbol{\varrho}_k \mid \mathbf{x}_k^i) \tag{11}$$

be a particle description of the total likelihood function. Whereas the likelihood function based on pseudoranges is directly given by solving (8) for each particle

$$p(\boldsymbol{\varrho}_k \mid \mathbf{x}_k^i) \sim \mathcal{N}(\boldsymbol{\varrho}_k; 0, \sigma_\epsilon^2). \tag{12}$$

But recalling section III-C, $p(\mathbf{s}_k \mid \mathbf{x}_k)$ is not defined on the continuous state space $\mathbf{X}$, so a particle approximation is not easily obtained. For that reason, an additional approximation between the discrete space $\check{\mathbf{X}}$ and the continuous space $\mathbf{X}$ is proposed. The solution for the likelihood based on RSSI tuples, is as follows: Carry out the fingerprint database correlation (9) for each particle $\mathbf{x}_k^i$ instead of each fingerprint entry $\bar{\mathbf{p}}_k^m$. In doing so, the database entry, which is closest in $\mathbb{R}^3$ to the current particle position, is found via

$$\hat{m} = \arg\min_m(||\mathbf{p}_k^i - \bar{\mathbf{p}}_k^m||),$$

and its respective RSSI tuple is exploited, $\mathbf{s}^i \leftarrow \mathbf{s}^{\hat{m}}$ to compute the so-called particle database correlation. The obtained particle correlation result is assigned as the new, updated weight to the particle. Repeating this procedure for each particle gives

$$p(\mathbf{s}_k \mid \mathbf{x}_k^i) = \int_{\mathcal{S}} \frac{1}{\sqrt{2\pi}\sigma_\kappa} \exp\left(-\frac{1}{2}\left(\frac{\mathbf{s}_k - \hat{\mathbf{s}}^i}{\sigma_\kappa}\right)^2\right) \mathrm{d}\mathbf{s}, \tag{13}$$

which is the particle representation of the RSSI pseudo-likelihood. Even though the RSSI tuples used for the particle database correlation do not stand exactly for the signal strength at the particle position,

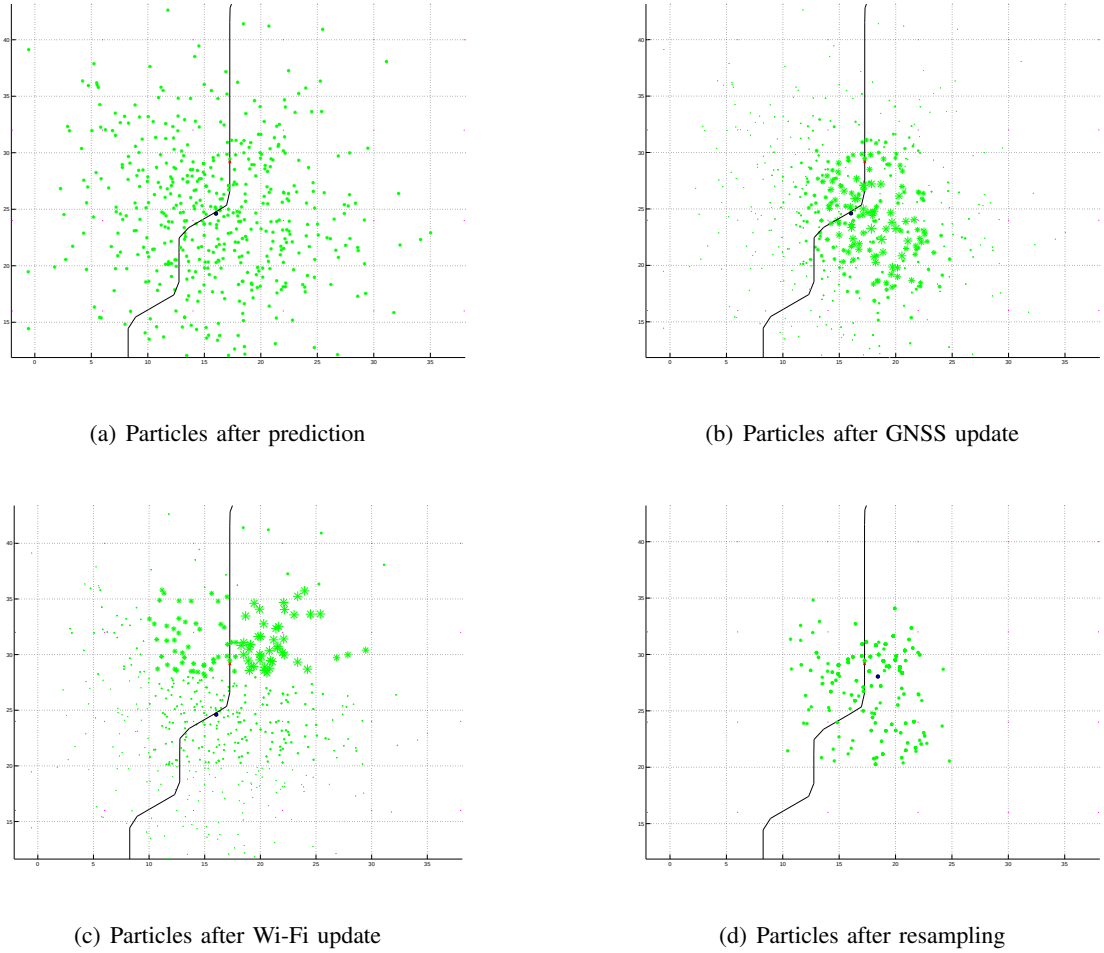

(a) Particles after prediction

(b) Particles after GNSS update

(c) Particles after Wi-Fi update

(d) Particles after resampling

Fig. 1. Particle cloud propagating through the different steps of the algorithm: Beginning with the prediction of the particles in (a), followed by a correction with pseudoranges in (b) and/or with RSSI in (c). Resulting in the posterior PDF (d) after resampling.

this approximation is reasonable when contemplating the fluctuation of RSSI readings in realistic Wi-Fi environments. The errors, due to this approximation are within that range of random changes within Wi-Fi measurements. Due to the algorithm, the same RSSI tuple and, consequently, the same weight may be assigned to several particles. This fact supports the idea of regular resampling, explained below. Normalising (12) and (13), if required, allows finally to fuse the two likelihood functions by means of multiplying the updated particle weights.

As mentioned, a resampling step is executed after each recursion of the SIR particle filter, to avoid the degeneracy problem. Several resampling strategies might be possible. In general, resampling is a scheme of redrawing particles according to their weights. Now, the distribution of the particles approximates the posterior PDF $p(\mathbf{x}_k \mid \mathbf{z}_{1:k})$, and to all particles equal weights $1/N$ are assigned. As mentioned before, the position estimate can be achieved by e.g. taking the conditional mean of the posterior PDF.

A complete cycle of the Bayesian recursion is depicted in figure 1. The distributions can be seen at different steps of the Bayesian recursion, approximated by the particles. Particles which were weighted high by the measurement updates, are depicted larger. (a) shows the particle distribution after it propagated through the process model. It is almost Gaussian distributed. Afterwards the particle distribution is weighted by the pseudorange measurements (b), which also results in a Gaussian distribution and by the RSSI measurements (c), resulting in a distribution according to shadowing effects. The result obtained by applying both sensor updates and resampling can be found in (d).

V. Simulation Results

A. Experimental Setup

This section presents the results of the experiments conducted, based on the "Spirent Communications" (Spirent, n.d.) GNSS signal generator and "MATLAB®" MATLAB (n.d.) simulations. Properties which were investigated are the absolute positioning errors for different scenarios and the joint estimation of the GNSS user clock offset. Furthermore, the ability of the algorithm will be shown to continue the position estimation with less than 4 satellites, and even with a complete outage of one of the systems.

In all experiments which are presented, the same trajectory of the MU was used, with the same sets of Wi-Fi AP and the same regular grid of Wi-Fi fingerprints. It is necessary to mention that the fingerprint grid points were only 2-dimensional and their distance to each other was 8 m. The particle filter was run with 1000 particles. The experiments were repeated 500 times, and the results were averaged respectively. The data rate at which the measurements were obtained was set for both systems to 1 s. GNSS pseudoranges were simulated using "SimGEN" (Spirent, n.d.) software. If not mentioned otherwise, the number of satellites was 8. The Wi-Fi fingerprint database was generated as described in (Seitz *et al.* , 2010a), and the Wi-Fi RSSI readings, too. Considering the grid distance of fingerprints, and the experience with awiloc® (awiloc, n.d.), the simulated Wi-Fi environment approximates rather an outdoor scenario. Filter parameter for the measurement likelihoods are set to $\sigma_\kappa = 8\,\text{dB}$ and $\sigma_\varepsilon = 5\,\text{m}$. The standard deviation σ_κ mainly addresses the relatively large grid point distance, rather than the variation of RSSI readings. To get a particle distribution to initialise the filter, a uniform distribution over the whole local coordinate system was generated.[1]

B. Simulations

The first result, which can be seen in figure 2, serves as an overview of the simulation scenario and as a proof of concept, since these simulations were done without any errors nor any extra shadowing for Wi-Fi signals. Almost all results compare the Wi-Fi and GNSS standalone particle filter estimates with the estimates computed by the data fusion algorithm. It is observable that the result obtained by the combination of the two sources lies in between the GNSS pseudorange solution and the Wi-Fi solution. This behaviour can be modified by adapting the variances of the filter likelihood functions. The deviation of Wi-Fi positions from the true positions is about 3 m (ignoring up-coordinate), and is primary caused by the fingerprint grid point distances. The root-mean-square-error (RMSE) of these position estimates can be found in figure 3 including the estimated user clock offset. In the 4th plot of figure 3 the ability of the filter to estimate the user clock offset can be seen. Furthermore, a convergence of the filter is visible after about 20 s. This a slow convergence caused by the data rates of 1 s. A data rate for pseudoranges is usually higher, up to 20 Hz, which allows the filter to converge faster. The subfigures above depict the RMSE of the estimates for each coordinate. In subfigure 3, the RMSE of the up-coordinate is depicted, which is, in the case of the Wi-Fi standalone solution, exceptionally high. This is due to the generation of radio maps based on local 2D maps, where the up-coordinate is usually constant. So, after the filter initialisation, the up-coordinate of standalone Wi-Fi is constant, too. Here, GNSS pseudoranges measurements were able to improve the accuracy of a Wi-Fi fingerprinting positioning system and decreased the RMSE to about half a meter in that kind of ideal case. The up-coordinate estimate of the proposed algorithm is always approximately equal the up-coordinate estimate of the GNSS only solution.

In the following is presented, the total RMSE of the same simulation, with extra uncorrelated Gaussian noise added to the measurements. It should be mentioned, that our Wi-Fi simulation environment is simulated with random shadowing effects instead of solid obstacles and fluctuation. In particular zero mean noise with standard deviation of 3 dB was added to the RSSI, and with standard deviation of 5 m to the pseudoranges. In table I the reader may observe the advantage of the presented data fusion scheme. The proposed algorithm is more precise than standalone solutions, and outperforms them by 1 m total RMSE. The more accurate position estimates in the noisy scenario can be explained by the additional information each of the systems provides for the other system.

Figure 4 presents the results of a more diversified scenario. Again the noiseless scenario is used. This

[1]The initialisation was done in each of the 500 runs. Therefore all simulations may differ a bit albeit they are averaged over 500 runs.

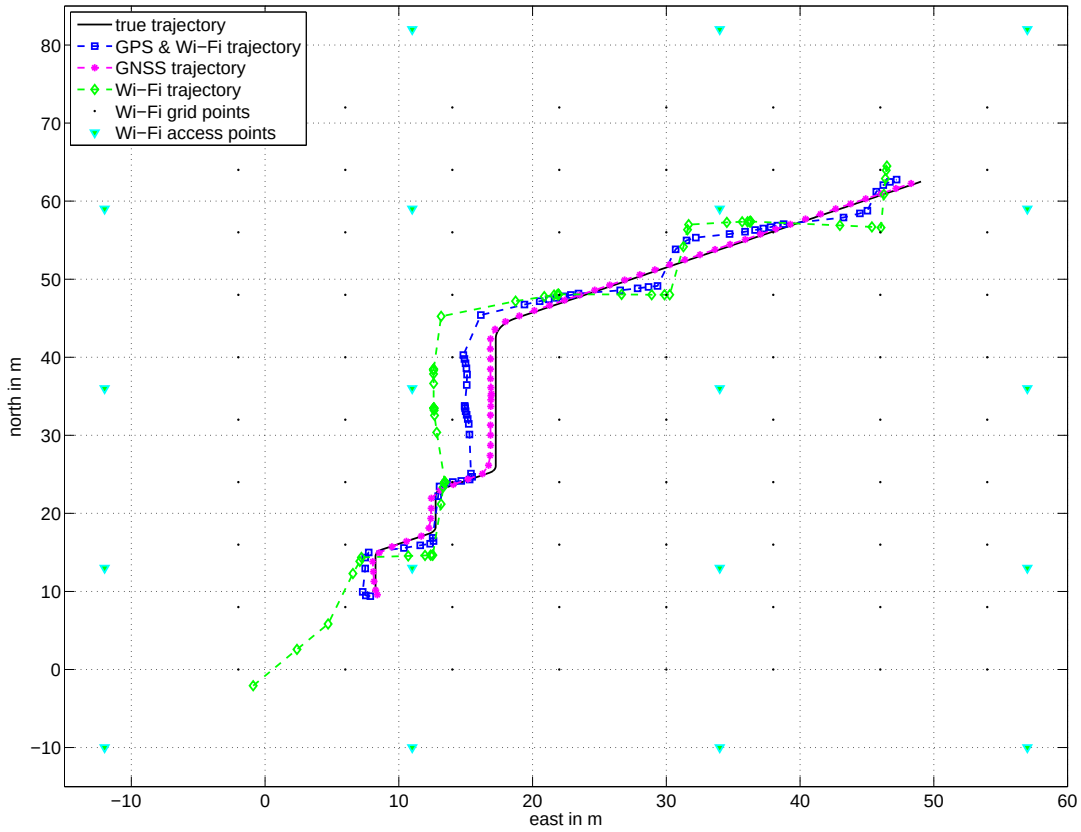

Fig. 2. Position estimates in 2D of standalone GNSS, of standalone Wi-Fi and of the proposed fusion of GNSS & Wi-Fi in comparison to ground truth. Added are the fingerprints and the Wi-Fi access points.

time the number of satellites is stepwise reduced, followed by an outage of pseudoranges of 10 s to which, after 5 s, a Wi-Fi outage with a duration of 10 s was simulated. During the interval of $[25, 29]$ s the number of available satellites was set to 3 and afterwards in the period of $[30, 34]$ s it was set to 1. In the first three subfigures, the RMSE for each axis can be seen. Below in subfigure 4, the total RMSE is shown. The last subfigure depicts the number of satellites as orientation. The vertical lines mark the outage periods of GNSS pseudoranges and Wi-Fi RSSI. In subfigure 3 the periods of constant errors attract attention. It can be explained due to insufficient number of satellites during that period, so the up-coordinate cannot be estimated anymore and the process model, which does not assume motion in any direction. As stated before, the up-coordinate for the Wi-Fi only solution is not estimated anyways. When looking at the total error of standalone GNSS, it increases after 30 s, which continues during the GNSS outage interval. After the 46th second, the pseudoranges outage ends and the GNSS error returns to its original error level. The error of the GNSS & Wi-Fi, in the same plot, is smaller than the GNSS only error. It stays low between second 35 and

TABLE I
RMSE OF STANDALONE GNSS, OF STANDALONE WI-FI AND THE PROPOSED FUSION OF GNSS & WI-FI OF EACH COORDINATE AXIS AND IN TOTAL.

RMS position error	east/m	north/m	up/m	total/m
standalone GNSS	2.52	5.24	3.56	6.82
standalone Wi-Fi	5.82	3.64	20.83	21.93
GNSS & Wi-Fi	2.46	4.35	3.11	5.89

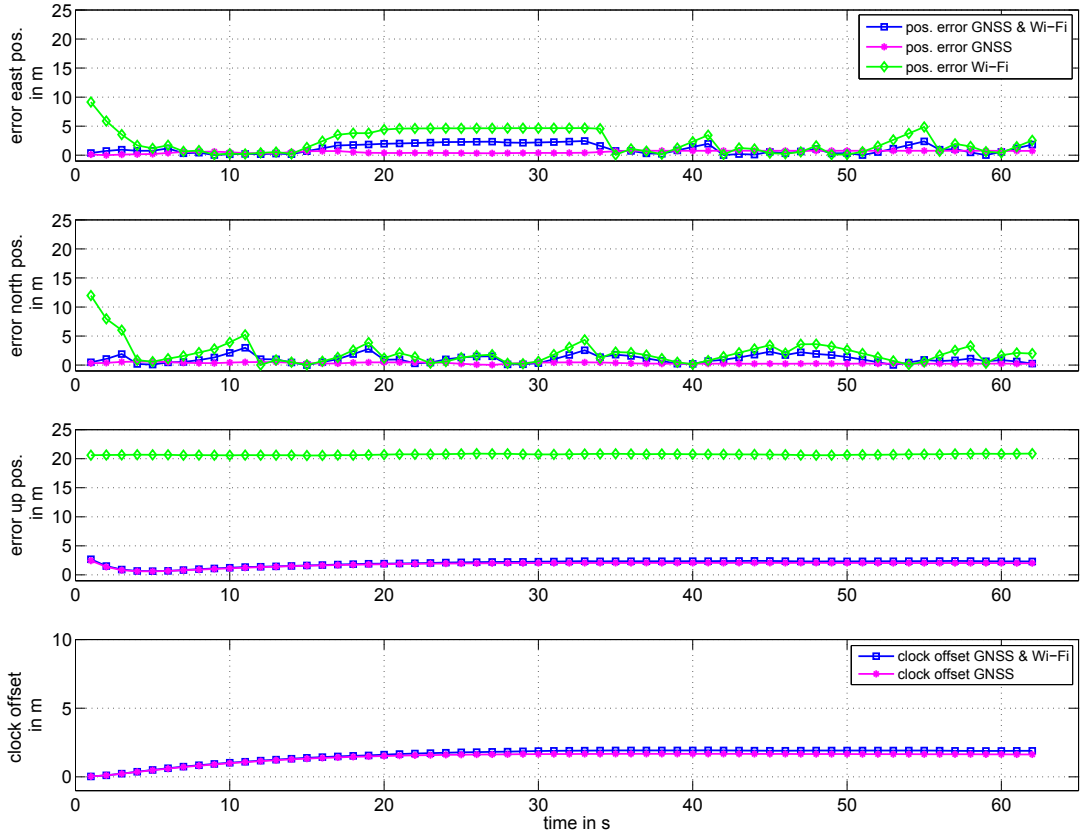

Fig. 3. RMSE of east, north and up-coordinate for standalone GNSS, of standalone Wi-Fi and of the proposed fusion of GNSS & Wi-Fi and the estimated GNSS user clock offset for standalone GNSS and GNSS & Wi-Fi.

40 and rises after the Wi-Fi outage starts at second 40. Needless to say, the Wi-Fi only error rises during the Wi-Fi RSSI outage interval.

VI. Conclusion

A flexible algorithm is presented to fuse GNSS pseudoranges and Wi-Fi database correlation results. Two different sensor models, a GNSS pseudorange model and a Wi-Fi RSSI model, were set up to update the particle weights in the introduced SIR particle filter. Three-dimensional position and velocity are estimated together with the GNSS receiver clock offset. The algorithm can be seen as a Wi-Fi aided position, velocity and time determination algorithm (PVT) of a GNSS receiver.

The concept has been proved with simulation data. The fused estimates achieve a higher positioning accuracy than the standalone systems. The systematic altitude error of Wi-Fi positioning, due to the discrete fingerprinting database, can be compensated. GNSS and Wi-Fi outages can be bridged. On the one hand, through the use Wi-Fi database correlation results, the algorithm can deal with less than four satellites, on the other hand using GNSS pseudoranges, Wi-Fi positioning ambiguities can be solved. Hence is the algorithm more robust than the standalone systems and facilitates seamless navigation.

An analysis of different grid distances and the mapping of discrete Wi-Fi fingerprint data to continuous particles, will be left as a future work. A compensation of multipath propagation of GNSS signals needs to be integrated in the GNSS pseudorange model. Furthermore, the behaviour of the estimation with less than four satellites in view should be deeper investigated. Finally, an evaluation with measurement data collected in different environments will proof the usability of the proposed approach for seamless navigation.

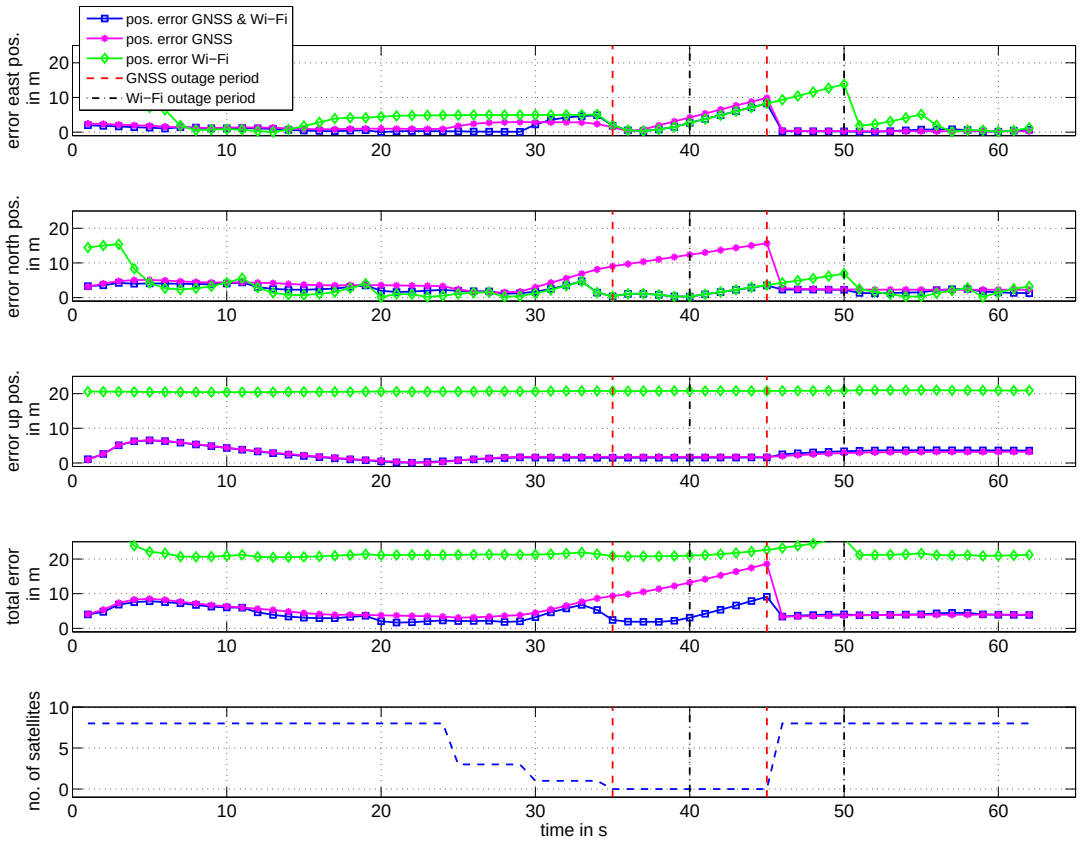

Fig. 4. RMSE of east, north and up-coordinate and the norm of the RMSE. All plots contain the result for standalone GNSS, for standalone Wi-Fi and of the proposed fusion of GNSS & Wi-Fi. The last plot shows the number of satellites. Outage intervals are marked with dashed and dash-dotted lines.

VII. Acknowledgements

This work has been done under the supported of the Bavarian ministry of economic affairs, infrastructure, transport and technology in the scope of the strategic program “Bayern 2020”. The author would like to thank the group Multi-Sensor-Systems of Fraunhofer IIS for their cooperation.

References

Arulampalam, M.S., Maskell, S., Gordon, N., & Clapp, T. 2002. A tutorial on particle filters for online nonlinear/non-Gaussian Bayesian tracking. *Signal Processing, IEEE Transactions on*, **50**(2), 174 –188.

awiloc. *awiloc is a registered trademark of the Fraunhofer Institute for Integrated Circuits IIS, Germany, 2010*. www.awiloc.com.

Bahl, P., & Padmanabhan, V.N. 2000. RADAR: an in-building RF-based user location and tracking system. vol. 2.

Bradford, P.W., Spilker, J., & Enge, P. 1996. *Global positioning system: theory and applications*. Vol. 109.

Eck, D., Schilling, K., Abdul-Majeed, A., Thielecke, J., Richter, P., Boronat, J.G., Schens, I., Thomas, B., Williger, B., & Lang, F.R. 2012. Mobility assistance for older people. *Applied Bionics and Biomechanics*.

Gordon, N.J., Salmond, D.J., & Smith, A.F.M. 1993. Novel approach to nonlinear/non-Gaussian Bayesian state estimation. *Radar and Signal Processing, IEE Proceedings F*, **140**(2), 107 –113.

Khider, Mohammed, Jost, Thomas, Abdo Sanchez, Elena, Robertson, Patrick, & Angermann, Michael. 2010 (may). Bayesian multisensor navigation incorporating pseudoranges and multipath model. *Pages 816 –825 of: Position Location and Navigation Symposium (PLANS), 2010 IEEE/ION*.

Li, B., Tan, Y.K., & Dempster, A.G. 2011. Using two global positioning system satellites to improve wireless fidelity positioning accuracy in urban canyons. *Communications, IET*, **5**(2), 163 –171.

MATLAB. *The MathWorks Inc., Natick, MA*.

Mok, E., & Lau, L. 2001. GPS vehicle location tracking in dense high-rise environments with the minimum range error algorithm. *Pages 2564–2570 of: Proceedings of the 14th International Technical Meeting of the Satellite Division of The Institute of Navigation (ION GPS 2001)*.

Mok, E., & Xia, L. 2005. Strategies for geolocation optimization in urban regions. *Pages 8–10 of: International Symposium on GPS/GNSS*.

Seitz, J., Vaupel, T., Meyer, S., Boronat, J.G., & Thielecke, J. 2010a (march). A Hidden Markov Model for pedestrian navigation. *Pages 120 –127 of: Positioning Navigation and Communication (WPNC), 2010 7th Workshop on*.

Seitz, J., Vaupel, T., Jahn, J., Meyer, S., Boronat, J.G., & Thielecke, J. 2010b (july). A Hidden Markov Model for urban navigation based on fingerprinting and pedestrian dead reckoning. *Pages 1 –8 of: Information Fusion (FUSION), 2010 13th Conference on*.

Shah, Z., & Malaney, R.A. 2006 (may). Particle Filters and Position Tracking in Wi-Fi Networks. *Pages 613 –617 of: Vehicular Technology Conference, 2006. VTC 2006-Spring. IEEE 63rd*, vol. 2.

Spirent. *Spirent*. www.spirent.com/.

Thrun, Sebastian, Burgard, Wolfram, & Fox, Dieter. 2006. *Probabilistic Robotics*. MIT Press.

Vermaak, J., & Blake, A. 2001. Nonlinear filtering for speaker tracking in noisy and reverberant environments. *Pages 3021 –3024 vol.5 of: Acoustics, Speech, and Signal Processing, 2001. Proceedings. (ICASSP '01). 2001 IEEE International Conference on*, vol. 5.

Wallbaum, M., & Wasch, T. 2004. Markov localization of wireless local area network clients. *Lecture Notes in Computer Science*, **2928**, 1–15.

Weyn, M., & Schrooyen, F. 2008. A Wi-Fi Assisted GPS Positioning Concept. *ECUMICT, Gent, Belgium*.

Wi-Fi. *Wi-Fi is a trademark of the Wi-Fi Alliance*. http://www.wi-fi.org.